Performance evaluation of FBMC versus OFDM in tapped delay line doubly selective channels

Ritesh Baranwal* and B.B. Tiwari

Department of Electronics Engineering,
VBS Purvanchal University,
Jaunpur, Uttar Pradesh, India
Email: riteshbaranwal01@gmail.com
Email: bbtiwari62@gmail.com
*Corresponding author

Abstract: As the technology grows in wireless communication, we move towards 5G. In mobile communication, this requires a greater number of users in limited bandwidth, and also the technology used is easily accessible to all. For these requirements, several types of research have been conducted to fulfil these requirements. To provide mobile service to all at a cheap rate a multicarrier modulation technique came into the picture and these multicarrier modulation techniques are used since 4G. An Orthogonal Frequency Division Multiplexing is used in 4G and some modifications in the Orthogonal Frequency Division Multiplexing signal are incorporated to make it suitable for 5G waveform technology. But requirements for 5G are very low out-of-band radiation, low Peak to Average Power Ratio, low reliability, and low latency communication, for enhanced mobile broadband. This paper investigates Filter Bank Multicarrier Modulation in time and frequency selective channels using Gabor Theory. Performance evaluation for the parameters like Bit Error Rate, Peak to Average Power Ratio, Power Spectral Densities for Filter Bank Multicarrier and Orthogonal Frequency Division Multiplexing in various real-time doubly selective channels TDL-A, TDL-B, TDL-C, pedestrian channel, vehicular channel as suggested by the Third Generation Partnership Project has been done.

Keywords: 5G; Python; FBMC; OFDM; PHYDYAS; vehicular; TDL channel.

Reference to this paper should be made as follows: Baranwal, R. and Tiwari, B.B. (2023) 'Performance evaluation of FBMC versus OFDM in tapped delay line doubly selective channels', *Int. J. Wireless and Mobile Computing*, Vol. 24, No. 1, pp.1–8.

Biographical notes: Ritesh Baranwal received his BTech degree in Electronics and Instrumentation Engineering from VBS Purvanchal University, Jaunpur, Uttar Pradesh, India in 2007 and MTech degree in Communication Engineering from the University of SHUATS, Allahabad (now Prayagraj), India in 2012. He achieved Silver Medal in MTech. Currently, he is an Assistant Professor in the Department of Electronics Engineering at VBS Purvanchal University, Jaunpur (222003), India since 2008. His research interests include wireless communication, OFDM and signal processing.

B.B. Tiwari received his MSc (Physics) and MTech (E & C Engineering) degrees from the University of Roorkee (now IIT, Roorkee), India and PhD degree from the Institute of Engineering & Technology, Lucknow, India in 1984, 1986 and 1993, respectively. He is a Professor of Electronics Engineering specialising in Photonics and Optical Communication. Currently, he holds the position of Head of the Department of Electronics Engineering, Dean, Faculty of Engineering & Technology and the Director, Institute of Pharmacy at VBS Purvanchal University, Jaunpur, India. He has published his research works in reputed journals of the world and has been supervising PhD Scholars in the area of Optical Communication, Wireless Communication and VLSI Technology. He is Fellow of the Institution of Engineers (India) and Fellow of the Institution of Electronics & Telecommunication Engineers (India) Member IEEE, and other professional bodies.

1 Introduction

A lot of researches are going on in the field of Wireless Communication. One of the concerns is to assign a suitable waveform for studies in 5G (Andrews et al., 2014; Shafi et al., 2017; Huawei, 2021). In 4G LTE Orthogonal Frequency Division Multiplexing (OFDM) signal is used but this waveform does not have good time-frequency localisation as there exists out of band leakage and less spectral efficiency. Moreover, the Third Generation Partnership Project (3GPP) has decided to stick with OFDM. Therefore, a waveform Filter Bank Multicarrier (FBMC) (Farhang-Boroujeny, 2011) comes into the picture. An FBMC is one of the waveforms which obeys the orthogonality principle as in OFDM used in 4G LTE. It is obtained by convolution of the signal received at the receiver with the impulse response of the wireless channel so that the signal obtained at the receiver antenna is orthogonal. There exist many types of FBMC (Nissel et al., 2017) but in this paper, we highlight the Offset Quadrature Amplitude Modulation (OQAM) because it provides good spectral efficiency. Staggered multitone and cosine-modulated multitone is the other name for OQAM (Bölcskei, 2003; Nissel and Rupp, 2016). An FBMC waveform is used which practices proper time-frequency signal to utilise efficiently available Time-Frequency Resources (Sejdić et al., 2009). Also, the low delay spread assures that a simple one-tap equaliser is sufficient to achieve optimal performance. Therefore, throughout our simulation one-tap equaliser is used. FBMC has a high Peak to Average Power Ratio (PAPR) (Na et al., 2021) and is approximately similar to that of OFDM. Performance (Na et al., 2021; Liu et al., 2016; Gerzaguet et al., 2017) of OFDM with FBMC in various real-time Rayleigh fading doubly selective channels (3GPP, 2018) TDL-A, TDL-B, TDL-C, Pedestrian Channel and Vehicular Channel using Gabor theory. The TDL Channel, Pedestrian Channel and Vehicular Channel (El-Ganiny et al., 2021) mode is designed by 3GPP. From our simulation studies the results are presented in Figures 5 to 15. The numerical value of various parameters like Peak to Average Power Ratio (PAPR), Spectral Efficiency (Marina et al., 2020) and Bit rate for OFDM, FBMC (Khudhair1 and Singh, 2020) in the TDL-A channel are also calculated. Monte Carlo simulation is used to validate the results.

This paper is organised as Section 2 talking about multicarrier modulation in OFDM. A brief description of Filter Bank Multicarrier is given in Section 3. Simulation parameters are given in Section 4. Results and Discussion are presented in Section 5. Finally, the Conclusion and Reference are given in Sections 6, 7 respectively.

2 Multicarrier modulation in OFDM

In a single carrier modulation, single-carrier data occupies the entire Communication bandwidth B. This single carrier system experience Inter Symbol Interference (ISI) due to full utilisation of entire bandwidth B and this bandwidth B is greater than coherence bandwidth. Figure 1 shows the transmission in Multi-Carrier modulation (NPTEL, 2021) system with subcarrier spacing B/N. Here, the whole Bandwidth B is divided into N sub-carriers. So, the bandwidth of each sub-carrier is B/N. This sub-carrier bandwidth B/N is smaller than coherence bandwidth, so each sub-carrier experiences frequency flat fading. Hence there is no ISI in the time domain. In multicarrier modulation, the data transmitted in parallel is less prone to data loss as compared to single carrier modulation. However, the symbol rates for MCM and single carrier transmission are the same. The mathematical expression for *i*-th sub-carriers transmitted in bandwidth B/N of Figure 1 is

$$V_i\left(t\right) = X_i \mathrm{e}^{j2\pi F_i t} \tag{1}$$

where X_i is the data transmitted on the *i*-th sub-carrier. F_i is the centre frequency of *i*-th sub-carrier bandwidth in which $F_i = \mathrm{i}\frac{B}{N}$. The value of *i* lie in the range $\left(-\frac{N}{2}-1\right) \le \mathrm{i} \le \frac{N}{2}$ and *N* is the number of sub-carriers. The total carrier data *V*(*t*) is sum of these sub-carrier data $V_i\left(t\right)$ which is represented by (2). The time instant of the *U*-th sample is represented by (3).

$$V\left(t\right) = \sum_{i=-\left(\frac{N}{2}-1\right)}^{\frac{N}{2}} V_i\left(t\right) \rightarrow V\left(t\right) = \sum_{i=-\left(\frac{N}{2}-1\right)}^{\frac{N}{2}} X_i e^{j2\pi i\frac{B}{N}t} \tag{2}$$

Figure 1 Multi-carrier modulation sub-carriers

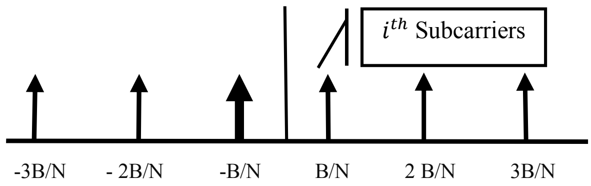

It is the sample of multi-carrier modulation signal/IDFT of information symbols. It is obtained by considering the time *t* instant of the *U*-th sample represented by $t = U$. T_s in which sampling time $\left(T_s\right) = \frac{1}{B}$.

$$V\left(UT_S\right) = X\left(U\right) = \sum_{i=-\left(\frac{N}{2}-1\right)}^{\frac{N}{2}} X_i e^{j2\pi i\frac{B}{N}\frac{U}{B}}$$

$$X\left(U\right) = \sum_{i=-\left(\frac{N}{2}-1\right)}^{\frac{N}{2}} X_i e^{j2\pi\frac{w}{N}} \tag{3}$$

It is simply possible to generate a composite MCM transmit signal using Inverse Fast Fourier Transform (IFFT). This proposed scheme of generating the MCM transmit signal has much lower implementation complexity compared to using Bank of Modulators. This is termed OFDM. At the receiver to recover the information symbols, one can correspondingly employ a Fast Fourier Transform (FFT) operation.

3 Filter bank multi-carrier

FBMC employs a prototype filter that is localised in time and frequency (Nissel and Rupp, 2016). The time spacing, as well as frequency spacing, is reduced by using the Balian-Low theorem in which only real-valued symbols (Nissel and Rupp, 2016) are transmitted. Figure 2 shows the working of FBMC in which each sub-carrier of FBMC is passed through a PHYDYAS filter for pulse shaping. Then, after pulse shaping add all these sub-carriers. This is the FBMC signal. This signal then passed through a doubly selective channel. Some noise is generated in the FBMC signal when it passes through a doubly selective channel. After that this FBMC signal is recovered at the receiver. The output before the noise is shown in equation (4) which is an integral multiple of channel impulse response and prototype filter impulse response.

$$\hat{U}_i(f) = \int_{-\infty}^{\infty} H(f)\breve{A}_i(f)\,df \tag{4}$$

where, $\hat{U}_i(f)$ – Channel output, $\breve{A}_i(f)$ – Filter Impulse Response, $H(f)$ – Channel Impulse Response, $\delta_i(f)$ – Filter Phase Response, $\mu(f)$ – Channel Impulse Response.

For Inter Symbol Interference **(**ISI) free transmission of FBMC the *i*-th sample and time shifted version of *i*-th sample are orthogonal to each other which is represented by equation (5).

$$\int_{-\infty}^{\infty} \hat{U}_i(t)\hat{U}_i(t-KT)\,dt = 0 \text{ for } \forall \;\&\; K = \pm 1, \pm 2, \pm 3 \tag{5}$$

For Inter Carrier Interference (ICI) free transmission of FBMC the *i*-th sample and time shifted of *j*-th sample are orthogonal to each other which is represented by equation (6)

$$\int_{-\infty}^{\infty} \hat{U}_i(t)\hat{U}_j(t-KT)\,dt = 0 \text{ for } \forall\; i, j,\; i \neq j \;\& \quad K = \pm 1, \pm 2, \pm 3 \tag{6}$$

Figure 2 Block diagram of FBMC

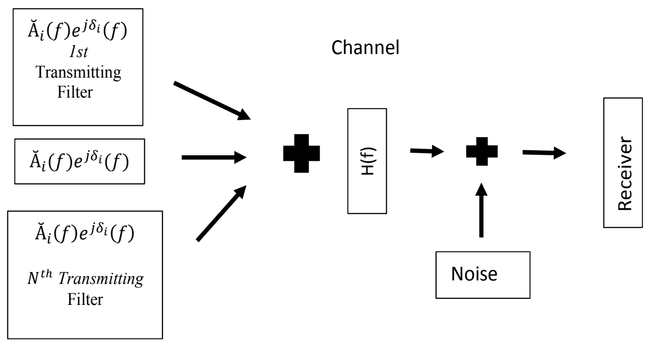

This way communication ISI and ICI interference can both be reduced simultaneously if the transmitting filters can be designed to the point where (5) applies to all *i* and (6) to all *i* and *j* $(i \neq j)$. This is FBMC's overarching structure. The FBMC waveform is based on Gabor's proposal (Feichtinger and Strohmer, 2021) in which a function can be expanded into a series of elementary functions which are constructed from a single building block by translation and modulation (transition in time and frequency domain). Let us denote sub-carrier position '*n*' and time-position '*k*' represented by the transmit data symbol $C_{k,n} \in Z$ with Z describing the symbol alphabet for QAM or PAM. The transmitted signal f(t) is the mathematical representation of FBMC, consisting of *N* sub-carrier and *K* time-symbol, shown below:

$$f(t) = \sum_{k=1}^{K}\sum_{n=1}^{N} C_{k,n}\,\hat{g}_{k,n}(t) \tag{7}$$

Where elementary function $\hat{g}_{k,n}(t)$ is time and frequency-shifted versions of the prototype filter $\hat{g}(t)$:

$$\hat{g}_{k,n}(t) = \hat{g}(t-k\bar{a})e^{j2\pi nb(t-k\bar{a})}e^{j\theta_{k,n}} \tag{8}$$

in which $\theta_{k,n}$ is phase shift which is equal to $\frac{\pi}{2}(k+n)$. Observe that time spacing '$\bar{a}b$' and frequency spacing 'b' determine the spectral efficiency.

3.1 Balian – Low theorem

With the parameter $\bar{a}$ and Ụ b which represent Time and Frequency shift, respectively, the pulse shape $\hat{g}_{k,n}(t)$ for $\bar{a}b$ = 1 for OFDM is given by the relation (Balian – Low Theorem)

$$\int_{-\infty}^{\infty} \left|\hat{g}_{k,n}(t)\right|^2 t^2 \int_{-\infty}^{\infty} \left|\hat{g}_{k,n}(\omega)\right|^2 \omega^2 = \infty \tag{9}$$

Based on the sampling density of the time-frequency lattice, a Gabor system can be classified as follows:

3.1.1 Oversampling

$\bar{a}b$ < 1: A frame that is well suited to localising time frequency information exists (particular examples are frames with Gaussian and appropriate oversampling rate).

3.1.2 Critical sampling

$\bar{a}b$ = 1: It is possible to create frames and orthonormal bases, but without good time-frequency understanding.

3.1.3 Under sampling

$\bar{a}b$ > 1: This would lead to an incomplete Gabor family. Mazo (1975) and PHYDYAS Project (2010) showed that communication in under sampling is also possible where sampling can be deceased until the Mazo limit is reached.

3.2 Modelling of prototype filters

In designing of FBMC system, there are certain parameters are considered to select the prototype filter. These are better Time-Frequency performance, higher spectral efficiency, low out of band leakage. So, a prototype filter named PHYDYAS filter (Das, 2018) is used to design FBMC in this paper. The impulse response of the PHYDYAS filter is as follows:

$$\hat{g}(t) = 1 + 2\ \hat{g} = 1 + 2\sum_{o=1}^{O-1} H_o^2\ Cos\left(2\pi\frac{ot}{OT}\right) \tag{10}$$

where o =0, 1, 2, 3,…,O.

where T is symbol period, O – Overlapping factor, o – symbol index. Table 1 shows the PHYDYAS filter frequency coefficient for different values of overlapping factor.

3.3 Filter pulse shaping (Farhang-Boroujeny, 2011)

A filter's impulse response ($\breve{A}_i(f)$) should be modelled in accordance with equation

$$\breve{A}_i^2(f)H^2(f) = Ci + \bar{Q}_i(f) > 0 \text{ for } f_i + f_{s/2} < f_i - f_{s/2} \quad (11)$$

In this case, C_i can be any arbitrary constant (real-data symbol) and the shaping function $\bar{Q}_i(f)$ has odd symmetry about $f_i + f_{s/2}$ and $f_i - f_{s/2}$. Figure 3 illustrates how to shape the amplitude characteristic of the pulse by passing it through Prototype Filter. The purpose of doing this is to make the signal fit in its frequency band. As part of FBMC, the signal is designed in such a way that at the receiver's end it is orthogonal. Consistent channels over a certain period are useful. Also, the phase $\delta_i(f)$, i=1, 2, 3…, N–1 should be shaped such that

$$\delta_i(f) - \delta_{i+1}(f) = \pm\pi/2 + \bar{\phi}_i(f) \quad (12)$$

Table 1 Coefficients of PHYDYAS filters for frequency domain

O	H_0	H_1	H_2	H_3
1	1	–	–	–
2	1	$\frac{\sqrt{2}}{2}$	–	–
3	1	0.911438	0.411438	–
4	1	0.9719598	$\frac{\sqrt{2}}{2}$	0.235147

where $\bar{\phi}_i(f)$ is an arbitrary phase with odd symmetry about $f_i + f_{s/2}$.

Figure 3 Transmitting prototype filters – shaping amplitude $\breve{A}_i(f)$ characteristics (Chang, 1966)

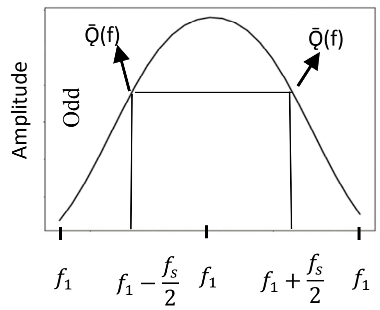

In FBMC the known channel transmitting filters can be designed such that it is free of ISI & ICI while attaining the maximum possible baud rate. However, this is designed for real data symbols only (Nissel and Rupp, 2017; Shibata et al., 2020).

4 PAPR

PAPR is the ratio of peak power to an average power of the signal and is calculated by using the relation (Baranwal et al., 20212).

$$\text{PAPR} = \frac{Pt_{peak}}{Pt_{Average}} \quad (13)$$

where

$$Pt_{\text{peak}} = \max_{0<t<MT} |V(t)|^2, \quad Pt_{\text{average}} = \frac{1}{MT}\int_0^{MT} |V(t)|^2$$

A power amplifier's input-output characteristic is illustrated in Figure 4. In this figure, if the peak deviation power of the waveform from its average power is higher than the linear range, the signal level is out of the linear range. As a result, high PAPR in OFDM and FBMC.

Figure 4 Power amplifier characteristic

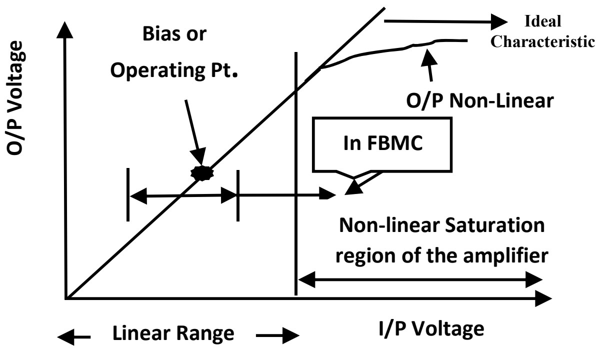

The high PAPR in an OFDM system essentially arises because of the IFFT operation. In IFFT the data symbols across sub-carriers can add up to produce a high-peak value signal.

But in FBMC high PAPR is due to filter pulse shaping characteristics, resulting in ICI and Cellular mobile batteries draining faster.

Table 2 Simulation parameter

S. No.	*Simulation parameter*	*Values*
1	No. of sub-carriers	256,512,1024
2	Carrier frequency	2.5 GHz
3	QAM order	16
4	Sub-carrier spacing in Hz	15 KHz
5	Sampling frequency	20.16 MHz
6	Number of Monte Carlo repetitions	100
7	Power delay profile (TDL-A, TDL-B, TDL-C)	300 ns
8	Power delay profile (Vehicular Channel, Pedestrian Channel)	370 ns, 44 ns

5 Results and discussion

For designing a filter bank multicarrier, most of the parameters are taken from 3GPP TR 38.901 (3GPP, 2018) specification in which they define Rayleigh fading channel profile for NLOS under the name TDL-A, TDL-B, TDL-C, Vehicular Channel, Pedestrian Channel are taken. This TDL mode is defined for the frequency range 0.5 to 100 GHz. Figure 5 compares the PAPR value of OFDM with FBMC. The PHYDYAS filter is used to create the FBMC and the overlapping factor is 4 taken in this paper. The Power spectral densities for TDL-A, TDL-B, TDL-C are shown in Figures 6, 7 and 8. These channels are doubly selective and it is found that FBMC has lower side lobes. This leads to an advanced utilisation of the allotted spectrum leading to higher spectral efficiency and low Out of Band (OOB) leakage when compared to OFDM as shown in Figures 6, 7 and 8.

Figure 5 Peak to average power ratio of FBMC & OFDM

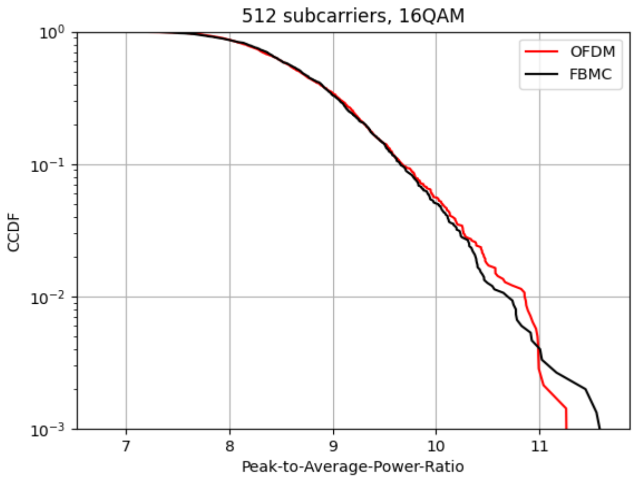

Figure 6 Power spectral density using PHYDYAS filter TDL – A

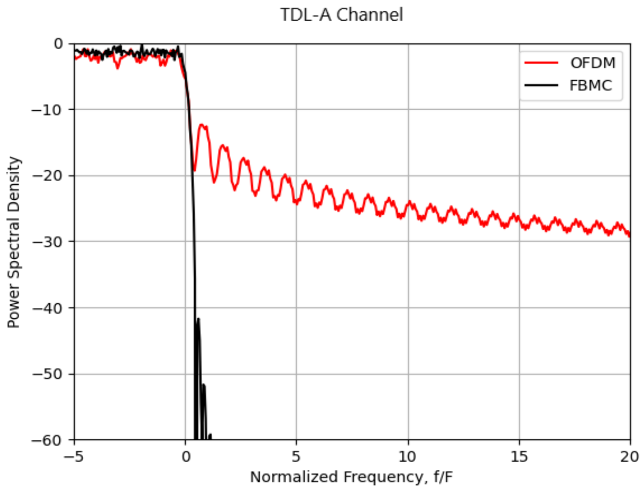

Figures 9, 10 and 11 show that BER decreases with increasing SNR for FBMC, OFDM with CP and OFDM (no CP) but BER in FBMC decreases rapidly as compared to OFDM (no CP).

Figure 7 Power spectral density using PHYDYAS filter TDL –B

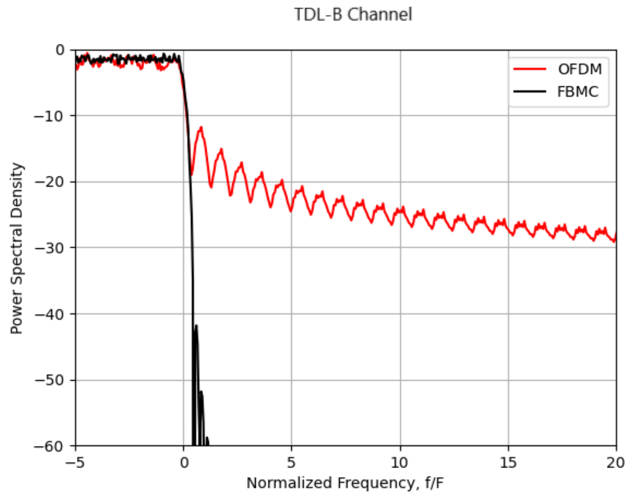

Figure 8 Power spectral density using PHYDYAS filter TDL –C

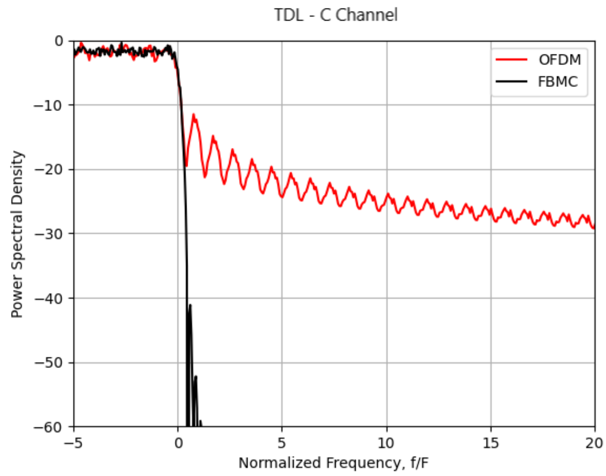

Figure 9 Bit error rate using PHYDYAS filter in TDL – A

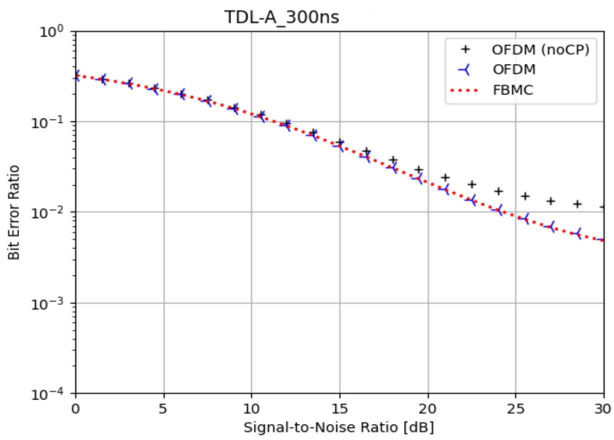

Figure 10 Bit error rate using PHYDYAS filter in TDL – B

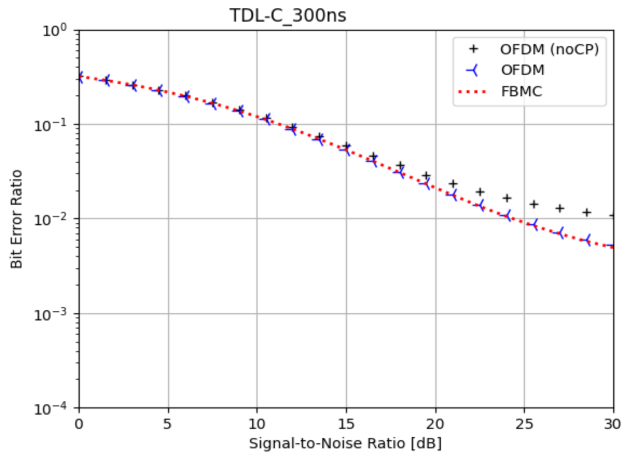

Figure 11 Bit error rate using PHYDYAS filter in TDL – C

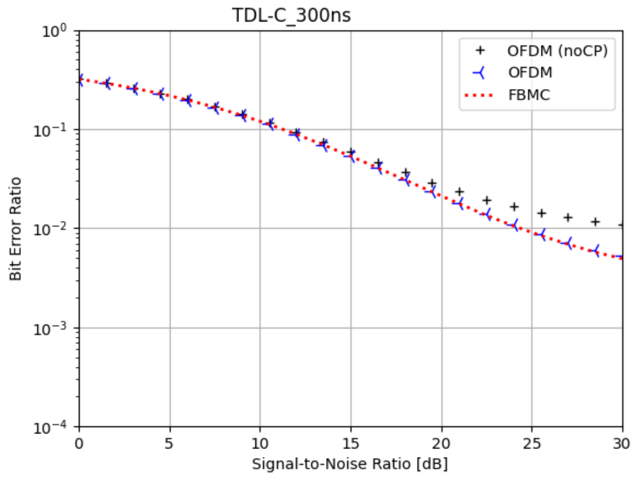

There is a very slight reduction in PAPR of FBMC than OFDM and it is 0.03 dB less for 512, 1024 sub-carriers as shown in Table 3. Figure 5 and Table 3 show that the PAPR of FBMC is approximately similar to the PAPR of OFDM.

Table 3 PAPR (dB) value at different sub-carriers

S. No.	*Waveforms*	*PAPR (dB) for N=256*	*PAPR (dB) for N=512*	*PAPR (dB) for N=1024*
1	OFDM	7.04	7.60	7.75
2	FBMC	6.99	7.57	7.72
Difference in PAPR value of OFDM, FBMC Waveform		0.05	0.03	0.03

A comparison of the Bit Rate, and Spectral Efficiency of OFDM, FBMC is shown in Table 4. In this table bit rates of FBMC are 1.03 Mbps, 2.05 Mbps and 4.1 Mbps higher than OFDM for 256, 512 and 1024 sub-carriers. So, the bit rate is more for FBMC than OFDM for the same number of sub-carriers. Also, the spectral efficiency of FBMC is 0.26 bits/sec./Hz higher than OFDM waveform for 256, 512 and 1024 sub-carriers. A doubly selective TDL-A channel is used to simulate the parameters of Table 4.

Table 4 Bit rate and spectral efficiency of OFDM, FBMC in TDL – A channel

S. No.	*No. of sub-carriers(N)*	*Parameters*	*OFDM*	*FBMC*	*Difference*
1	256	Bit Rate (mbits/sec)	14.33	15.36	1.03
		Spectral Efficiency (bits/sec/Hz)	3.73	4	0.27
2	512	Bit Rate (mbits/sec)	28.67	30.72	2.05
		Spectral Efficiency (bits/sec/Hz)	3.73	4	0.27
3	1024	Bit Rate (mbits/sec)	57.34	61.44	4.1
		Spectral Efficiency (bits/sec/Hz)	3.73	4	0.27

The power spectral density of FBMC and OFDM is compared in Vehicular and Pedestrian Channels as shown in Figures 12 and 13. It is found that FBMC has lower side lobes than those in OFDM leading to a high-spectral efficiency of FBMC. Figures 14 and 15 show that BER decreases with increasing SNR for FBMC, OFDM with CP & OFDM (No CP), but for FBMC BER is decreased more than OFDM (no CP) for the Vehicular Channel as compared to Pedestrian Channel. All these simulations are performed in python 3, and FBMC is the most suitable choice for 5G.

Figure 12 Power spectral efficiency using PHYDYAS filter in vehicular channel

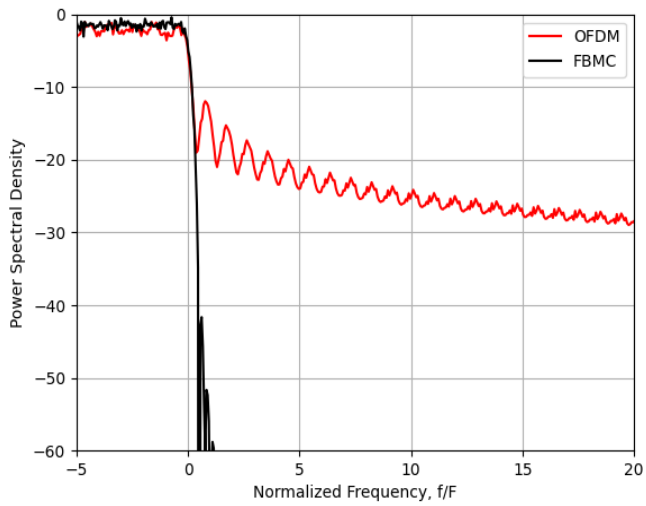

Figure 13 PSD using PHYDYAS filter in pedestrian channel

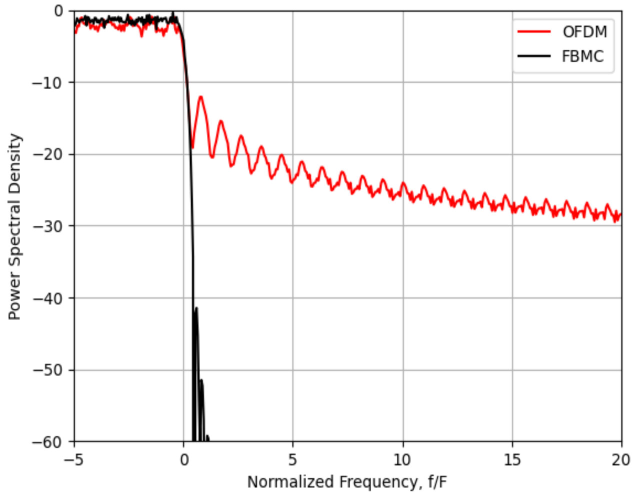

Figure 14 Bit error rate using PHYDYAS filter in pedestrian channel

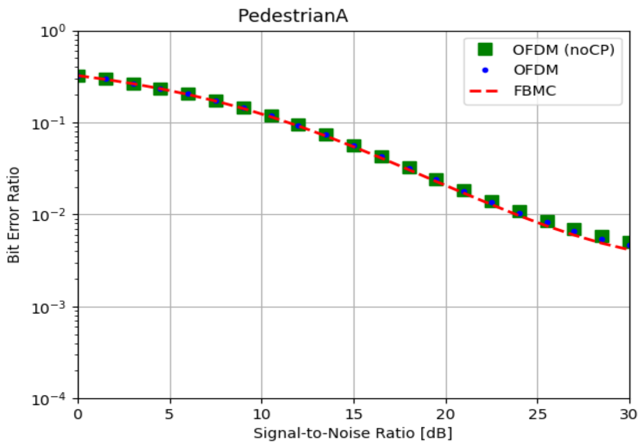

Figure 15 Bit error rate using PHYDYAS filter in vehicular channel

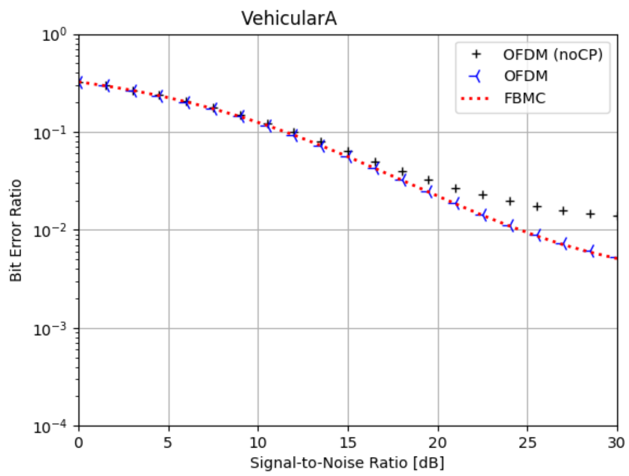

6 Conclusions

We have analysed to a great deal Filtered OFDM, Window OFDM and UFMC which have high spectral efficiency for a large number of users. But this is not practicable for the real-world scenario where there is a fluctuating number of users. For this reason, FBMC is useful which has high spectral efficiency for fluctuation. It has some advantages like low out of band leakage and lower side lobes, hence it has high-spectral efficiency, high-bit rate, low BER and better resilience to carrier frequency offset than OFDM. Based on all simulations done in this paper, we find that FBMC appears to be the best contender for future wireless communication, especially 5G communications. FBMC has addressed and removed the shortcomings of OFDM. It is an evolution of OFDM technology. Furthermore, all the simulations are performed due to a vast library of Python like NumPy, SciPy, matplotlib, etc. This Python is available free of cost, and there are a lot of scopes to reduce PAPR to still lower values.

Like OFDM, FBMC has a high PAPR. There are several techniques like Selective Mapping (SLM) with phase rotation, Partial Transmit Sequence (PTS) and SC-FDMA (DFT Spread OFDM) in OFDM to reduce PAPR value in which further studies can be carried on. It is possible to use these techniques for FBMC.

References

3GPP (2018) *Study on Channel Model for Frequencies from 0.5 to 100 GHz*, 3rd Generation Partnership Project (3GPP). Available online at: https://www.etsi.org/deliver/etsi_tr/138900_138999/138901/14.00.00_60/tr_138901v140000p.pdf (Accessed on 15 February 2021).

Andrews, J. G. et al. (2014) 'What will 5G be?', *IEEE Journal on Selected Areas in Communications*, Vol. 32, No. 6, pp.1065–1082.

Baranwal, R., Kumar, A. and Jaiswal, A.K. (2012) *Performance evaluation of different phase rotation on OFDM signal*. Ijsrp.org. Available online at: http://www.ijsrp.org/research_paper_may2012/ijsrp-may-2012-22.pdf (accessed on 4 March 2021).

Bölcskei, H. (2003) *Orthogonal Frequency Division Multiplexing based on Offset QAM' in Advances in Gabor Analysis*, Birkhäuser Boston, Boston, MA, pp.321–352.

Chang, R.W. (1966) 'Synthesis of band-limited orthogonal signals for multichannel data transmission', *The Bell System Technical Journal*, Vol. 45, No. 10, pp.1775–1796.

Das. S.S. (2018) *School of Telecommunications IIT Kharagpur: Evolution of Air Interface Towards 5G*. Available online at: https://nptel.ac.in/courses/108/105/108105134

El-Ganiny, M.Y. et al. (2021) 'A preamble based channel estimation methods for FBMC waveform: A comparative study', *Procedia Computer Science*, Vol. 182, pp.63–70.

Farhang-Boroujeny, B. (2011) 'OFDM versus filter bank multicarrier', *IEEE Signal Processing Magazine*, Vol. 28, No. 3, pp.92–112.

Feichtinger, H.G. and Strohmer, T. (2021) *Theory and Applications*, *Gbv.de*. Available online at: http://www.gbv.de/dms/ilmenau/toc/233462724.pdf (accessed on 2 April 2021).

Gerzaguet, R. et al. (2017) 'The 5G candidate waveform race: a comparison of complexity and performance', *EURASIP Journal on Wireless Communications and Networking*, No. 1. Doi: 10.1186/s13638-016-0792-0.

Huawei (2021) *5G-advanced technology evolution from a network perspective*. Available online at: https://wwwfile.huawei.com//media/CORP2020/pdf/event/1/5G_Advanced_Technology_Evolution_from_a_Network_Perspective_2021_en.pdf

Khudhair1, S.A. and Singh, M.J. (2020) 'Review in FBMC to enhance the performance of 5G networks', *Journal of Communication*, 15, pp. 415–426.

Liu, Y. et al. (2016) 'Waveform candidates for 5G networks: analysis and comparison', *arXiv [cs.IT]*. Available online at: http://arxiv.org/abs/1609.02427 (accessed on 10 June 2021).

Marina, P., Isnawati, A. and Afandi, M. A. (2020) 'Performance analysis of FBMC O-QAM system using varied modulation level', *Journal Infotel*, Vol. 12, No. 2, pp.45–51.

Mazo, J.E. (1975) 'Faster-than-nyquist signaling', *The Bell System Technical Journal*, Vol. 54, No. 8, pp.1451–1462.

Na, D. et al. (2021) 'Field trials of SC-FDMA, FBMC and LP-FBMC in indoor sub-3.5 GHz bands', *Electronics*, Vol. 10, No. 5. Doi: 10.3390/electronics10050573.

Nissel, R. and Rupp, M. (2016) 'On pilot-symbol aided channel estimation in FBMC-OQAM', *Proceedings of the IEEE International Conference on Acoustics, Speech and Signal Processing (ICASSP)*, IEEE, pp.3681–3685.

Nissel, R. and Rupp, M. (2017) 'OFDM and FBMC-OQAM in doubly-selective channels: calculating the bit error probability', *IEEE Communications Letters: a Publication of the IEEE Communications Society*, Vol. 21, No. 6, pp.1297–1300.

Nissel, R., Schwarz, S. and Rupp, M. (2017) 'Filter bank multicarrier modulation schemes for future mobile communications', *IEEE Journal on Selected Areas in Communications*, Vol. 35, No. 8, pp.1768–1782.

NPTEL (2021) *NPTEL, electronics & communication engineering – advanced 3G and 4G wireless mobile communications*. Available online at: https://nptel.ac.in/courses/117/104/117104099/ (accessed on 5 May 2021).

PHYDYAS Project (2010) *Ict-phydyas.org*. Available online at: http://www.ict-phydyas.org (accessed on 7 march 2021).

Sejdić, E., Djurović, I. and Jiang, J. (2009) 'Time – frequency feature representation using energy concentration: an overview of recent advances', *Digital Signal Processing*, Vol. 19. No. 1, pp.153–183.

Shafi, M. et al. (2017) '5G: a tutorial overview of standards, trials, challenges, deployment, and practice', *IEEE Journal on Selected Areas in Communications*, Vol. 35, No. 6, pp.1201–1221.

Shibata, L., Müller, F. and Klautau, A. (2020) *Open-Source Python Package for 5G MIMO Processing*, *Org.br*. Available online at: https://www.sbrt.org.br/sbrt2020/papers/1570661423.pdf (accessed on 22 April 2021).